

Absorption spectroscopic studies of carbon dioxide conversion in a low pressure glow discharge using tunable infrared diode lasers

F Hempel¹, J Röpcke¹, F Miethke² and H-E Wagner²

¹ Institut für Niedertemperatur-Plasmaphysik, Friedrich-Ludwig-Jahn-Str. 19,
17489 Greifswald, Germany

² Institut für Physik, Ernst-Moritz-Arndt Universität Greifswald, Domstr. 10 a,
17489 Greifswald, Germany

Received 9 March 2001, in final form 15 April 2002

Published 27 May 2002

Online at stacks.iop.org/PSST/11/266

Abstract

The time and spatial dependence of the chemical conversion of CO₂ to CO were studied in a closed glow discharge reactor ($p = 50$ Pa, $I = 2\text{--}30$ mA) consisting of a small plasma zone and an extended stationary afterglow. Tunable infrared diode laser absorption spectroscopy has been applied to determine the absolute ground state concentrations of CO and CO₂. After a certain discharge time an equilibrium of the concentrations of both species could be observed. The spatial dependence of the equilibrium CO concentration in the afterglow was found to be varying less than 10%. The feed gas was converted to CO more predominantly between 43% and 60% with increasing discharge current, forming so-called quasi-equilibrium states of the stable reaction products. The formation time of the stable gas composition also decreased with the current. For currents higher than 10 mA the conversion rate of CO₂ to CO was estimated to be 1.2×10^{13} molecules J⁻¹. Based on the experimental results, a plasma chemical modelling has been established.

1. Introduction

The volume chemistry of non-equilibrium plasmas is of growing interest, in particular, in relation to the field of treatment and cleaning of exhaust fumes of power stations, lorries or cars. The online monitoring of the stable plasma reaction products in chemical reactors, in particular the measurement of their ground state concentrations, is the key to an improved understanding of the plasma chemistry and the kinetics in these molecular discharges. This can be done, e.g., by diagnostic methods using absorption spectroscopy.

Tunable diode laser absorption spectroscopy (TDLAS) in the mid-infrared spectral region between 3 and 20 μm is a non-invasive technique for measuring number densities of stable molecules and radicals. TDLAS can also be used to determine neutral gas temperatures [1] and to investigate dissociation processes [2–5]. Due to their small laser line width (about 10⁻⁴ cm⁻¹) the lead-salt diode lasers used in the mid-infrared region are well suited for high resolution

spectroscopy purposes, e.g. of low molecular weight free radicals and molecular ions [6–9].

One of the most successful applications of TDLAS is for studying the decomposition of hydrocarbons in a variety of PECVD processes. Recently, systematic investigations of plasma chemistry and kinetics in plasmas containing hydrocarbons have been published [2, 10]. Outside of plasma diagnostics this technique has been used successfully in the field of atmospheric trace gas monitoring and for exhaust gas monitoring of on-road vehicles, e.g. [11–13].

The TDLAS allows also time resolved measurements with repetition rates exceeding 1 kHz. Recently, a new compact and transportable TDLAS system for plasma and gas phase process diagnostics and control has been developed, that works with four independent diode lasers simultaneously and millisecond time resolution [14].

Within the last decades, the kinetics of the CO₂ chemistry has been in the centre of interest of several studies. Absorption spectroscopic methods, using diode lasers in the near- [15–18]

and mid-infrared region [19–21], have been applied to monitor concentrations of CO and CO₂ in the combustion of burner flames under atmospheric and low pressure conditions. These measurements were performed with temporal resolutions between some milliseconds [18] and some minutes [21]. Giacobbe *et al* [22] monitored for industrial manufacturing applications the production of CO in a plasma arc reactor at high temperatures from carbon dioxide flowing under atmospheric conditions over carbon powder. Morvova [21] studied the development with time of the conversion chemistry in dc corona discharges of CO/air and CO₂/air mixtures using a FTIR absorption spectrometer. Recently, Kylian *et al* [23] investigated the time evolution and the steady state of the CO₂ decomposition in dc glow discharges in sealed-off CO₂ laser mixtures by means of time-resolved optical emission spectroscopy.

The work presented in this paper is based on publications of Rutschler *et al* [24], Lucke *et al* [25], Sonnenfeld *et al* [26] and Gundermann *et al* [27]. Sonnenfeld *et al* [26] monitored plasma chemical processes in different low pressure non-thermal gas discharge systems (dc positive column, hf) containing CO₂ using gas chromatography. Their experimental investigations were focused on the establishment of so-called chemical quasi-equilibrium states in two different reactor types: the flow reactor (divided in an active zone and a passive zone) and the closed system (temporally combination of plasma phase and relaxation phase). The gas analysis was performed by extracting gas samples in the temporal afterglow of the discharge. In addition, they discussed a basic kinetic model of the CO₂/CO/O₂ conversion chemistry. Gundermann *et al* [27] determined the electron density in CO₂/CO/O₂ mixtures in the dc positive column under similar plasma conditions, studied here, using microwave diagnostic methods.

In the present paper, the plasma chemical decomposition of CO₂ is studied in a further kind of closed reactor, characterized by a stationary active zone, separated in space and surrounded by a stationary afterglow. The investigations were focused on tunable diode laser absorption spectroscopic studies in the mid-infrared region, which had been performed in the extended stationary afterglow of a closed dc glow discharge of CO₂. For the first time, absolute concentrations of CO and CO₂ were measured time and spatially resolved in such a low pressure discharge system to monitor the temporal development of the chemical conversion process in the CO₂/CO/O₂ system. From these data, conversion rates were estimated in dependence on the discharge current. A basic model of the reaction kinetics has been established to obtain further insight. The results of the model matched the measured temporal developments for CO₂ and CO.

2. Experimental

The experimental set-up of the used absorption spectroscopy system and the discharge system is shown in figure 1.

The small plasma zone and the long extended stationary afterglow were located in a closed stainless steel vacuum chamber of 48 cm × 30 cm × 6 cm. Figure 2 shows a schematic side view of the vessel. The cylindrical discharge electrodes (7) are made from aluminium with a diameter of 1 cm. The current

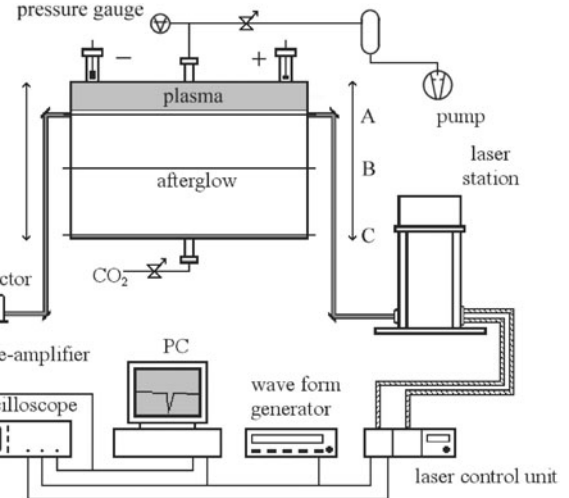


Figure 1. Experimental set-up with measurement positions (A, afterglow near the discharge; B, centre of the afterglow; C, end of the afterglow).

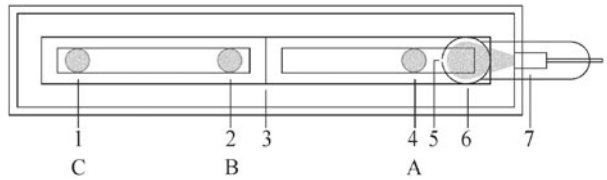


Figure 2. Schematic side view of the discharge vessel (1, measurement position C at the end of the afterglow 22 cm from the slit; 2, measurement position B in the centre of the afterglow 12 cm from the slit; 3, centre supporting part for the KBr windows; 4, measurement position A in the afterglow near the discharge 1 cm from the slit; 5, side view of the 1 mm slit in the discharge tube; 6, discharge tube; 7, cylindrical aluminium discharge electrodes).

of the dc glow discharge varied between 2–30 mA. The discharge area, in particular the positive column was located in a glass tube (6), which had a diameter of 3 cm and a length of 48 cm. This glass discharge tube was connected to the two electrodes and located at one wall of the chamber. The tube had a small lateral slit (5) of 1 mm width over the whole length at the tube wall to the open chamber. The afterglow filled the rest of the discharge vessel. The centre supporting part (3) was necessary to fix the windows to the metallic vessel.

Before generating the plasma, the discharge vessel was filled with CO₂ at an initial pressure of 50 Pa. Then the volume was closed, the plasma was ignited and the temporal development of the molecular species concentration was observed. The pressure in the chamber was found to increase related to the CO₂ conversion to CO. After stopping the discharge and the measurement, the system was evacuated to a pressure of less than 0.01 Pa before refilling. Measurements were repeated five times and averaged.

For the time and spatially resolved tunable infrared diode laser absorption spectroscopic measurements in the afterglow of the discharge a TDLAS system built by Muetek Infrared Laser Systems with two infrared lead-salt diode lasers was used. The diode lasers were mounted in a laser station with a helium closed cycle cryostat (see figure 1). The temperature of the lasers could be controlled at milli-Kelvin precision in the range between 25 and 80 K. The infrared laser beam

Table 1. Molecular absorption lines used for line identification and concentration measurements.

Molecule line	Line position (cm ⁻¹)	Line strength (cm/molecule)	References	Remarks
CO (1)	2073.2646	9.087×10^{-20}	[28]	Used for measurements
CO (2)	2073.4892	6.640×10^{-22}	[28]	Used for identification
CO (3)	2073.5252	3.990×10^{-21}	[28]	Used for identification
CO ₂	617.1895	2.302×10^{-21}	[28]	Used for measurements

passed a grating monochromator that servers as a mode filter (not shown in figure 1) before entering the discharge chamber via KBr windows located on two sides of the vessel. The absorption length of the single pass through the discharge vessel was 48 cm. The laser beam position in the plasma reactor could be adjusted using a set of moveable optical mirrors. Measurements were performed at three different positions, (A) 1 cm away from the exit slit of the discharge tube, (B) in the centre region of the afterglow in 12 cm distance to the slit and (C) at the end of the afterglow 22 cm from the slit of the discharge tube. The laser signal was recorded using an infrared detector mounted in a liquid nitrogen dewar. The absorption signal of the detector was amplified and transferred to a PC system. In addition, the spectra could be visualized using a Tektronix TDS 714L digital oscilloscope.

The diode laser was driven with a rectangular pulse of a frequency of 2.5 kHz provided by a HP 33120A waveform generator. The data acquisition was performed using a SPECTRUM 12 bit PAD1232 A/D-converter transient recorder board in the PC system with a sample frequency of 30 MHz. Data processing was realized by a software routine named DENSIDET for basic processing of the absorption spectroscopic data. A time resolution of three seconds was chosen for the measurements of the temporal development of the CO and CO₂ concentration, lasting five minutes.

The absorption lines of CO and CO₂ used for concentration measurements and line identification, their absolute positions and line strengths are listed in table 1. A representative direct tunable diode laser absorption spectrum measured nearby the slit of the discharge tube with three lines due to CO is shown in figure 3. For the measurements of the CO concentration line (1) was used. In this wavenumber region at plasma on conditions, it was possible to observe a hot band of excited CO in the afterglow of the discharge too (not shown in figure 3).

The identification of the absorption lines and the measurement of their absolute positions was carried out using the wavenumber calibration of the grating monochromator of the spectrometer, well documented reference gas spectra, gas cells containing reference gases with known pressures and purity and an etalon of known free spectral range for wavenumber interpolation [28–30]. With the DENSIDET data output of the intensity ratio I/I_0 the species density was easy to calculate using Lambert–Beer’s law. Based on the profile and intensity analysis of the CO absorption lines with and without a discharge a gas temperature of about 350 ± 50 K could be estimated. This observation is in accordance with the rather low power input of about 30 W in maximum into the discharge, leading to an only slight heating of the discharge vessel of about 10–20 K above room temperature.

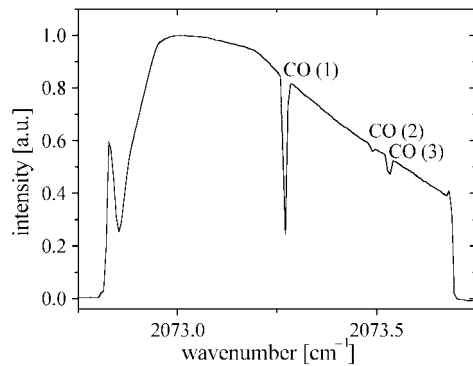


Figure 3. Example of a TDL absorption spectrum with three CO lines in the 2073 cm⁻¹ wavenumber region (see table 1) measured at 1 cm distance from the discharge tube (position A, pulsed diode, $f = 2.5$ kHz).

3. Results and discussion

3.1. Investigation of the temporal development

Figure 4 shows the measured temporal development of the CO concentration during the CO₂ conversion process at the different positions in the afterglow of the dc glow discharge with a discharge current of 30 mA. For clarity reasons not every measured point is shown in this figure.

As one can see, the temporal development and the equilibrium value of the concentration of CO did not depend on the measuring position in the afterglow of the discharge for a given pressure and discharge current within the accuracy of measurements. The equilibrium value of the product concentration was reached at the same time near the plasma zone, in the middle of the afterglow as well as at the end of the afterglow. The slightly reduced CO equilibrium concentration found at the end of the afterglow was still within the error bars. This result can be explained under the given experimental conditions by the relative large diffusion coefficient of about $50 \text{ cm}^2 \text{ s}^{-1}$ for the species transport along the chamber. A change in the species concentration in the active plasma zone led to a steady state in some tenth of a second in the whole chamber. For this reason, each small concentration gradient vanished in the afterglow part of the chamber faster than it could be detected with a time resolution of three seconds used for the measurements at the various positions.

In figure 5, the time dependence of the CO concentration in the centre of the afterglow is shown for four discharge currents. Again, for a better view, not all measured values are visualized. In agreement with former investigations [24–26], the formation of quasi-equilibrium CO concentration values, depending insignificantly on the current, was found. The

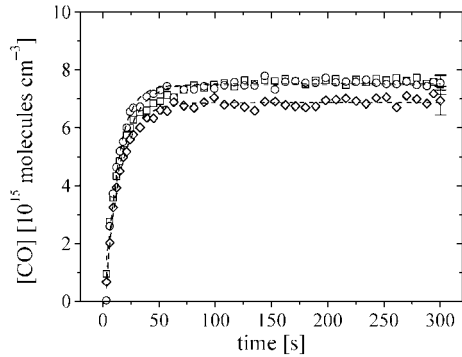


Figure 4. Time dependence of the CO concentration for the three different positions in the afterglow (not every measured point shown for clarity, $I = 30\text{ mA}$, \square : near the discharge (A), \circ : centre of the afterglow (B), \diamond : end of the afterglow (C)).

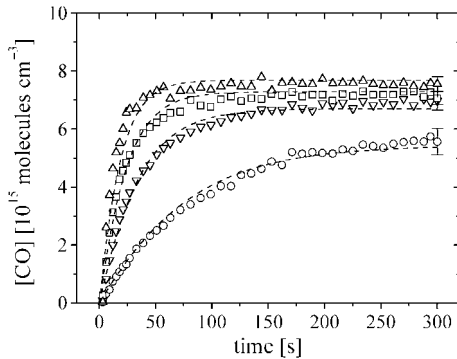


Figure 5. Comparison of the measured temporal developments of the CO concentration (symbols) with results of a numerical modelling of the chemical conversion kinetics (---) for four different discharge currents (not every measured point shown for clarity, centre position (B), \triangle : 30 mA, \square : 20 mA, ∇ : 10 mA, \circ : 2 mA).

graphs illustrate also the strong dependence of the formation time of the stationary species composition in the reactor on the discharge current. With increasing current, the number of CO molecules produced per time unit in the first seconds of the discharge built up. This led to a reduced time necessary to reach the equilibrium product composition.

The temporal developments of the CO concentration could be fitted for the various currents by exponential functions (not shown in figure 5):

$$[n] = [n]_E - A_1 \exp\left(\frac{t}{t_1}\right).$$

These fits gave values for the equilibrium concentrations $[n]_E$ and characteristic time constants t_1 which described the time necessary for the formation of a stationary product composition in the afterglow. Due to the fact that the starting concentration of CO is zero, $[n]_E$ and A_1 are equal. Figure 6 shows the small linear rise of the equilibrium concentration value $[n]_E$ and the strong exponential decrease of the formation time constant t_1 with increasing discharge current for measurements of the temporal development of CO in the centre of the afterglow. The numerical results for the equilibrium concentration $[n]_E$ and the formation time constant t_1 are given in table 2. With the density of the CO_2 before starting the plasma of about

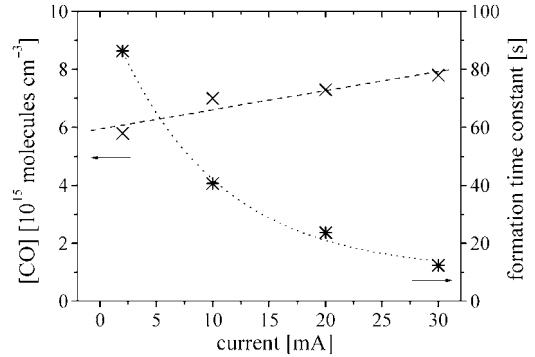


Figure 6. Results of exponential fitting of the measured temporal developments of the CO concentrations as a function of the discharge current (centre position (B), \times : equilibrium concentration value (left axis), $*$: formation time constant (right axis)).

$13 \times 10^{15} \text{ molecules cm}^{-3}$ and the equilibrium concentration values, one can calculate a final conversion ratio. This is listed in table 2, too. The increase of the equilibrium concentration values of CO and of the related final conversion ratio was mainly caused by the larger energy input into the discharge. This influences the chemical balance established in the plasma and in the spatial afterglow.

In the first seconds of running, the discharge the concentration of CO increased almost linearly with time. Depending on the power consumption of the plasma one could estimate a value for a conversion rate in the CO_2/CO discharge system, i.e. the number of CO_2 to CO converted molecules per energy value. The results of this estimation are also listed in table 2. In figure 7, the conversion rate is shown together with the values of the power input into the discharge. The input power on the two electrodes increased linearly with the current. The conversion rate was for currents higher than 10 mA estimated to be $1.2 \times 10^{13} \text{ molecules J}^{-1}$. For lower currents (such as 2 mA) the estimated conversion rate was twice as large as for currents of 10–30 mA. This means, on the one hand, that the energy efficiency of the conversion process for low currents was improved. On the other hand, since the input power was much lower it needed a longer time to establish a chemical equilibrium in the conversion process. It should be noted that at a low discharge current of 2 mA, the discharge characteristics differed considerably from conditions at all higher currents. Changed plasma properties, in particular a changed electron energy distribution function, could be considered as the reason.

A comparison of the time dependences of the CO and the CO_2 concentration in the centre of the afterglow is given in figure 8 for a discharge current of 20 mA. It was found that the concentration of CO_2 decreased in the same time scale of about 24 s as the density of CO increased. The mass balance could be considered as nearly fulfilled within the accuracy of the measurements. For this reason, the gas composition could be determined by knowledge either of the CO or the CO_2 concentration only.

3.2. Modelling

For further insight into the kinetics in the chemical conversion the measured temporal developments of the CO and the CO_2

Table 2. Equilibrium concentrations of CO and CO₂, formation time constants and conversion ratios, and rates derived by fitting the measured temporal developments in the centre of the afterglow and electron densities used in the model for various discharge currents. The electron density for 2 mA was taken from [27]. The values for the higher currents are linearly approximated.

Current (mA)	Molecule	Equilibrium concentration (molecules cm ⁻³)	Formation time constant (s)	Final conversion ratio (%)	Conversion rate (molecules J ⁻¹)	Electron density (cm ⁻³)
2	CO	5.8×10^{15}	86.3	43.6	2.58×10^{13}	2.6×10^9
10	CO	7.0×10^{15}	40.7	52.6	1.42×10^{13}	7.0×10^9
20	CO	7.3×10^{15}	23.7	54.9	1.19×10^{13}	1.1×10^{10}
	CO ₂	4.5×10^{15}	24.1	66.2	1.38×10^{13}	
30	CO	7.8×10^{15}	12.4	58.6	1.16×10^{13}	1.5×10^{10}

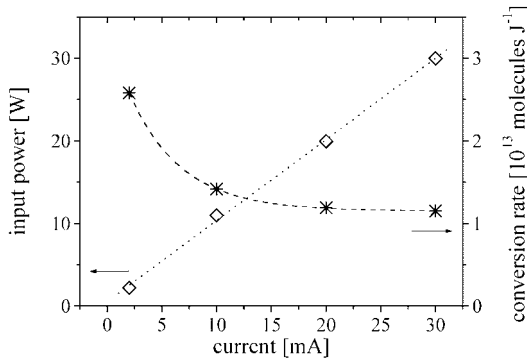


Figure 7. Input power and estimated conversion rate as a function of the discharge current (centre position (B), \diamond : input power (left axis), $*$: conversion rate (right axis)).

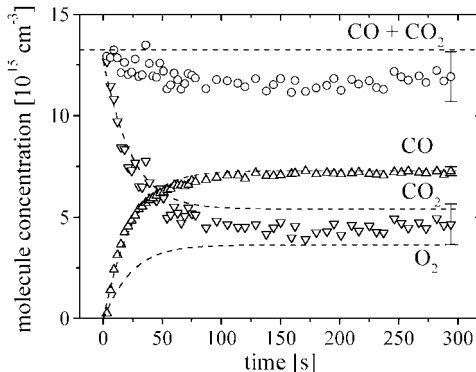


Figure 8. Comparison of the measured temporal developments of the CO and the CO₂ concentrations and its sum (symbols) with results of a numerical modelling of the chemical conversion kinetics (---) (not every measured point shown for clarity, centre position (B), $I = 20$ mA, ∇ : CO₂, Δ : CO, \circ : CO + CO₂).

concentrations in the centre of the afterglow of the discharge was modelled. For this purpose, the program package ‘FACSIMILE for Windows’ was used. FACSIMILE is a high-level programming language for solving ordinary differential equations in the field of science and engineering.

3.2.1. The basic model. A rather simple reaction scheme of 10 electron impact dissociation, wall-induced recombination and thermally activated reactions in the volume was used to model the kinetics of the chemical conversion process of CO₂ to CO. These reactions and their specific rate coefficients at a temperature of 350 K are given in table 3.

For the modelling of the kinetics of the conversion process only the most important reactions that decompose or produce CO₂, CO, C, O and O₂ were taken into account. The rate coefficients of electron impact dissociation reactions of CO₂ in discharges and wall-induced recombinations of species containing carbon were adapted related to other references like Sonnenfeld *et al* [26] or Mechold *et al* [31]. The rate equations for the thermally activated volume reactions were taken from Sonnenfeld *et al* [26], where a similar model is described. Sonnenfeld *et al* [26] assumed that due to the low ionization degree and the low discharge pressure reactions of excited neutrals and charged particles are of minor importance. These reactions were not included in the actual model. Other thermally activated volume reactions with small rate coefficients were also neglected in the model.

The value of the rate coefficient for the electron impact dissociation of CO₂ played a key role in the model. It influenced to a less extent the formation time of the conversion equilibrium but more seriously, it influenced the equilibrium concentration values of CO₂ and CO. Nevertheless, the rate coefficients used in this paper are smaller compared to Sonnenfeld *et al* [26]. The recombination to CO₂ on the wall seemed to be important for the formation time of the conversion equilibrium. The results of the measurements of the temporal development of the CO concentration at various positions in the afterglow showed no significant dependence on the distance to the active discharge (see figure 4). Therefore, the discharge vessel with the tube containing the plasma and the wide cavity filled with the stationary afterglow, where the measurements were made, was treated in the model like one big cell. No transportation and no diffusion effects in the chamber were taken into account since they had been proven to have no effect for the used time resolution (see above). Based on experiments, an estimated gas temperature of 350 K was used for the modelling of the chemistry. For the dissociation processes initiated by electron impact, an electron density of 1.1×10^{10} cm⁻³ was assumed for a discharge current of 20 mA. This value is in between the values used in [26] and [31]. The electron density of 2.6×10^9 cm⁻³ at 2 mA is in good agreement with the values measured by Gundermann *et al* [27] at this pressure in discharge tubes with the same diameter under comparable conditions, where for the reduced electric field a value of 28.17 V Torr⁻¹ cm⁻¹ and an averaged kinetic electron temperature of 1.1 eV was found.

For the starting concentration of CO₂ in the model, the first measured CO₂ density of 1.3×10^{16} molecules cm⁻³ was used. In figure 8, this value is shown as a dashed line to be compared with the summation of the measured concentrations

Table 3. Rate equations and rate coefficients of electron impact dissociation, wall recombination and thermally activated chemical reactions used to model the chemical conversion of CO₂ (*n*, number of reacting species; *n*_e, electron density) [26, 27].

No.	Reaction	Rate equation (cm ³ /molecule) ⁿ⁻¹ s ⁻¹)	Rate coefficient (cm ³ molecule ⁻¹ s ⁻¹)
1	CO ₂ + e ⁻ = CO + O + e ⁻		2.0 × 10 ⁻¹² n _e
2	CO + e ⁻ = C + O + e ⁻		5.0 × 10 ⁻¹³ n _e
3	O ₂ + e ⁻ = O + O + e ⁻		2.0 × 10 ⁻¹¹ n _e
4	CO + O + Wall = CO ₂ + Wall		2.0 × 10 ⁻¹⁵
5	O + O + Wall = O ₂ + Wall		1.1 × 10 ⁻¹¹
6	CO + O + M = CO ₂ + M	2.76 × 10 ⁻³² exp(-1764/T)	2.38 × 10 ⁻¹⁸
7	O + O + M = O ₂ + M	2.7 × 10 ⁻³² T ^{-0.5}	1.92 × 10 ⁻¹⁷
8	C + CO ₂ = CO + CO	1.74 × 10 ⁻¹³ T ^{0.5} exp(-1703/T)	2.32 × 10 ⁻¹⁴
9	C + O + M = CO + M	8.27 × 10 ⁻³² T ^{0.5}	5.88 × 10 ⁻¹⁷
10	C + O ₂ = CO + O	8.8 × 10 ⁻¹³ T ^{0.5} exp(-1661/T)	1.43 × 10 ⁻¹³

of CO and CO₂. The same density was used for the collision partner M in the calculation of the rate coefficients. In addition, it was assumed that the concentrations of the species produced in the discharge such as CO or O₂ were zero before starting the plasma.

3.2.2. Results of modelling. The results of modelling the measured temporal CO concentration behaviour (dashed lines) are presented for the four different discharge currents in figure 5 together with the measured development (symbols). To match the experimental data only the electron density in the model had to be altered. The values for the four different currents are given in table 2. The good agreement of the calculated temporal development and the measured behaviour for 2 mA, where the electron density from Gundermann *et al* [27] was used in the model, proved the validity of the used simple reaction scheme. Since the equilibrium concentration of CO depends only slightly on the electron density, the assumption of a fixed gas temperature would not seriously affect the results of the model. A difference of ±50 K in the gas temperature results in deviations in the order of the statistical error of the measurement. In figure 8, one can compare the modelled time dependence of the CO₂ and CO concentrations (dashed lines) with the measured behaviour (symbols) in the centre of the afterglow for a discharge current of 20 mA. In addition, the calculated value for the carbon content as the sum of the measured CO₂ and CO concentrations and the concentration behaviour of the molecular oxygen given by the model are shown. The equilibrium concentration of the atomic oxygen calculated by the model was about 8.7 × 10¹² molecules cm⁻³, the result for the carbon was 6.2 × 10¹⁰ molecules cm⁻³. Although various simplifications have been made for modelling the temporal concentration development the agreement of the experimental and modelling data is rather satisfying.

4. Summary

The time and spatial dependence of the chemical conversion of CO₂ to CO were studied in a closed glow discharge reactor (*p* = 50 Pa, *I* = 2–30 mA) consisting of a small plasma zone and an extended stationary afterglow by using tunable infrared diode laser absorption spectroscopy. The formation of a chemical quasi-equilibrium of both species could be observed. The spatial dependence of the equilibrium CO

concentration in the afterglow was found to be varying less than 10%. Between 43% and 60% of the CO₂ was converted to CO. The formation time of the stable gas composition decreased with the discharge current. The conversion rate of CO₂ to CO was estimated to be in the range of 10¹³ molecules J⁻¹. Based on the experimental results a rather simple plasma chemical model has been established.

Acknowledgments

The authors are indebted to L Mechold, M Käning and D Gött for helpful discussions and valuable technical assistance. Especially we are indebted to D Loffhagen for his support concerning the modelling. The project was partly supported by the Deutsche Forschungsgemeinschaft, Sonderforschungsbereich 198.

References

- [1] Haverlag M, Stoffels E, Stoffels W W, Kroesen G M W and De Hoog F J 1996 *J. Vac. Sci. Technol. A* **14** 380
- [2] Röpcke J, Mechold L, Käning M, Fan W Y and Davies P B 1999 *Plasma Chem. Plasma Process.* **19** 395
- [3] Davies P B and Martineau P M 1992 *Adv. Mater.* **4** 729
- [4] Naito S, Ito N, Hattori T and Goto T 1995 *Japan. J. Appl. Phys.* **34** 302
- [5] Haverlag M, Stoffels E, Stoffels W W, Kroesen G M W and De Hoog F J 1994 *J. Vac. Sci. Technol. A* **12** 3102
- [6] Kawaguchi K, Endo Y and Hirota E 1982 *J. Mol. Spectrosc.* **93** 381
- [7] Hunt N T, Röpcke J and Davies P B 2000 *J. Mol. Spectrosc.* **204** 120
- [8] Liu Z and Davies P B 1996 *J. Chem. Phys.* **105** 3443
- [9] Smith D M and Davies P B 1994 *J. Chem. Phys.* **100** 6166
- [10] Fan W Y, Knewstubb P F, Käning M, Mechold L, Röpcke J and Davies P B 1999 *J. Phys. Chem. A* **103** 4118
- [11] Nelson D D *et al* 1996 *SPIE Proceedings* **2834** 148
- [12] Jimenez J *et al* 1999 *J. Air Waste Manage. Assoc.* **49** 463
- [13] Schiff H I, Chanda A, Pisano J and Mackay G 1998 *Proc. SPIE—The International Society for Optical Engineering* **3535** 132
- [14] Röpcke J, Mechold L, Käning M, Anders J, Wienhold F G, Nelson D and Zahniser M 2000 *Rev. Scient. Instrum.* **71** 3706
- [15] Linnerud I, Kaspersen P and Jæger T 1998 *Appl. Phys. B* **67** 297
- [16] Mihalcea R M, Baer D S and Hanson R K 1997 *Appl. Opt.* **36** 8745

- [17] Mihalcea R M, Baer D S and Hanson R K 1998 *Meas. Sci. Technol.* **9** 327
- [18] Mihalcea R M, Webber M E, Baer D S, Hanson R K, Feller G S and Chapman W B 1998 *Appl. Phys. B* **67** 283
- [19] Daniel R G, McNesby K L and Mizolek A W 1996 *Appl. Opt.* **35** 4018
- [20] Schoenung S M and Hanson R K 1982 *Appl. Opt.* **21** 1767
- [21] Morvova M 1998 *J. Phys. D: Appl. Phys.* **31** 1865
- [22] Giacobbe F W and Schmerling D W 1983 *Plasma Chem. Plasma Processing* **3** 383
- [23] Kylian O, Leys C and Hrachova V 2001 *Contrib. Plasma Phys.* **41** 407
- [24] Rutscher A and Wagner H-E 1993 *Plasma Sources Sci. Technol.* **2** 279
- [25] Lucke W, Miethke F, Pfau S, Rutscher A and Wagner H-E 1993 *Proc. ISPC-11, Loughborough (England)* vol 3, p 1356
- [26] Sonnenfeld A, Strobel H and Wagner H-E 1998 *J. Non-Equilib. Thermodyn.* **23** 105
- [27] Gundermann S, Loffhagen, D, Wagner H-E and Winkler R 2001 *Contrib. Plasma Phys.* **41** 45
- [28] Rothman L S *et al* 1992 *J. Quant. Spectrosc. Radiat. Transfer* **48** 469
- [29] Guelachvili G and Rao K N 1986 *Handbook of Infrared Standards* (Orlando, FL: Academic)
- [30] Husson N *et al* 1994 *J. Quant. Spectrosc. Radiat. Transfer* **52** 425
- [31] Mechold L, Röpcke J, Käning M, Loffhagen D and Davies P B 1999 *Lausanne Report LRP* **629/99** 155